

Four layer monolithic integrated high T_c dc SQUID magnetometer

J. W. M. Hilgenkamp, G. C. S. Brons, J. G. Soldevilla, R. P. J. IJsselsteijn, J. Flokstra, and H. Rogalla

Department of Applied Physics, University of Twente, P. O. Box 217, 7500 AE Enschede, The Netherlands

(Received 31 January 1994; accepted for publication 11 April 1994)

$\text{YBa}_2\text{Cu}_3\text{O}_{7-x}$ based monolithic integrated dc SQUID magnetometers, consisting of a dc SQUID integrated with a flux transformer on a single bicrystalline substrate, have been fabricated and characterized. The devices consist of four layers, including two superconducting layers, and first realizations operate up to 73 K. A maximum voltage modulation of $32 \mu\text{V}$ is observed at 40 K. A field sensitivity of $0.17 \text{ pT}/\sqrt{\text{Hz}}$ is obtained above 200 Hz at 45 K and $0.49 \text{ pT}/\sqrt{\text{Hz}}$ at 1 Hz and 65 K.

To improve the field sensitivity of a high T_c SQUID (superconducting quantum interference device) magnetometer, the effective sensing area, defined as the ratio of the flux coupled into the SQUID and the applied magnetic field, can be increased by a flux focusing structure. Various configurations have been reported, such as a large area SQUID washer,¹ bulk flux concentrators,² and a large area shunt inductance parallel to the SQUID inductance.³ A more effective method is the classical one, to use a superconducting flux transformer consisting of a planar multiturn input coil connected to a (gradiometric) pickup inductance. The flux transformer is manufactured on a separate substrate (flip chip arrangement)⁴ or integrated monolithically with the SQUID on a single substrate,^{5,6} providing a tight coupling between the SQUID washer and the input coil. A monolithic integrated high T_c dc SQUID magnetometer, operating at 77 K, was first reported by Lee *et al.*,⁵ using template biepitaxial grain-boundary junctions. The device consisted of nine layers, including three superconducting layers. Reproducible fabrication, however, is much easier realized by using a lower number of layers. Kromann *et al.*⁶ reduced the number of layers to eight, including two superconducting layers, by using the SQUID washer as the return strip of the input coil.⁷ Using this concept, we have fabricated monolithic integrated high T_c dc SQUID magnetometers based on bicrystal grain-boundary junctions (see Fig. 1). The total number of layers has been further reduced to four, namely two superconducting $\text{YBa}_2\text{Cu}_3\text{O}_{7-x}$ (YBCO) layers, one insulating SrTiO_3 (STO) layer, and a Ti-Au contact layer. In the process, which can easily be adapted to other types of Josephson junctions, definition of the junctions is the last step. In this paper the design, fabrication, and electrical characteristics of the integrated dc SQUID magnetometers will be described.

In Fig. 2 a schematic cross section of the device is shown. The substrates used are (001) oriented SrTiO_3 bicrystals with a symmetric 24° [001] tilt grain boundary. First, gold markers are prepared by rf sputtering and lift-off to mark the boundary line. Then a 140 nm YBCO base layer is deposited by pulsed laser deposition (PLD)⁸ at a heater temperature of 790°C in a partial oxygen pressure of 30 Pa using a laser-pulse energy density of $1.3 \text{ J}/\text{cm}^2$. Layers prepared this way generally have T_c values above 88 K and a density of outgrowths (particles with typical dimensions of 200–300 nm) of less than 1 per $500 \mu\text{m}^2$. The SQUID

washer and the pickup loop are structured by standard photolithography and by Ar ion-beam etching,⁹ using an acceleration voltage of 500 V and a beam current of 10 mA, under an angle of 45° to obtain the smooth edges required to facilitate epitaxial growth of subsequent layers. Etching is performed intermittently (8 s on, 10 s off) to avoid heating of the sample. After removing the photoresist by acetone and alcohol, a 250 nm STO insulating layer is deposited by PLD at a heater temperature of 750°C in a partial oxygen pressure of 20 Pa using a laser-pulse energy density of $1.3 \text{ J}/\text{cm}^2$. The STO is removed above the IV contacts by Ar ion-beam etching and in a separate step, two edge contacts are structured, by which one end of the input coil is connected to the center of the washer and the other end to a terminal of the pickup loop. The other terminal of the pickup loop is connected directly to the washer. By Ar plasma etching a top layer of about 40 nm is removed from the sample, to provide a clean surface, before deposition of the 400 nm YBCO top layer takes place by PLD with the same deposition conditions as used for the base YBCO layer. Finally, Ti-Au contacts are prepared by rf sputtering and lift-off before the input coil is

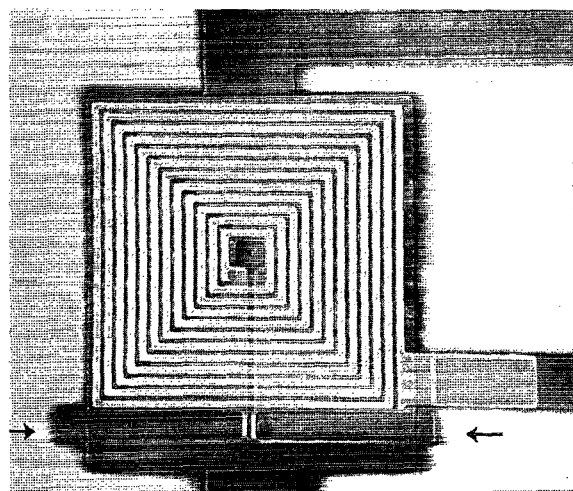


FIG. 1. Scanning electron microscope micrograph of the central part of the integrated dc SQUID magnetometer. The bicrystal grain boundary is indicated by the arrows. In the center the via contact connecting the input coil to the washer is visible.

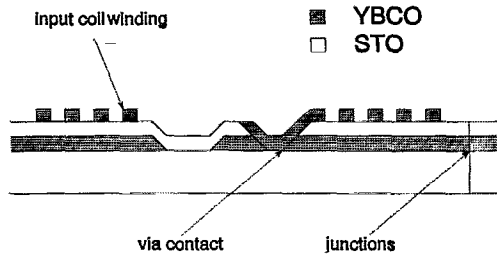


FIG. 2. Schematic cross section.

structured and the 5 μm wide junctions are defined by Ar ion-beam etching.

Three samples have been fabricated (A, B, and C). The most important design parameters are listed in Table I. A and B have an $11\frac{1}{2}$ turn input coil with 8 μm wide windings separated by 5 μm . The top layer of C was less smooth and we decided, therefore, to use a $6\frac{1}{2}$ turn input coil with 15 μm wide windings separated by 5 μm . In all samples the SQUID hole inductance is approximately 55 pH, and the slit inductance is about 70 pH. The square pickup loop has a side-length of 8.5 mm² and a width of 1025 μm .

Electrical characterization is performed in a variable temperature He gas-flow cryostat. Shielding from external noise sources is provided by a BiSrCaCuO pot with a critical temperature above 100 K mounted inside a mu-metal shield surrounded by an Al can. Noise measurements were performed in a flux locked loop using a 100 kHz square-wave flux modulation.

Due to a problem occurring during top layer deposition, the flux transformer of sample A did not function. Samples B and C operated up to about 73 K. For the Josephson junctions we measured $I_c R_n$ products of up to 0.3 mV at 15 K and a temperature-independent specific resistivity ρ_n of $5 \times 10^{-8} \Omega \text{ cm}^2$. Below about 20 K the IV curves show hysteresis. From this we calculated a specific junction capacitance of 0.2 Fm^{-2} . The voltage versus applied magnetic flux is shown for various bias currents at 45 and 65 K (sample C) in Figs. 3(a) and 3(b). The maximum voltage modulation we have measured was 32 μV at 40 K. The period of the modulation is approximately $1.8 \text{ nT}/\phi_0$. This corresponds to an effective sensing area of $A_{\text{eff}} = 1.2 \text{ mm}^2$. The flux transformer has increased the effective sensing area by a factor 78. For sample B the effective sensing area is increased by a factor 101. The period of modulation for this sample is $1.3 \text{ nT}/\phi_0$, corresponding to $A_{\text{eff}} = 1.6 \text{ mm}^2$. The measured results are in

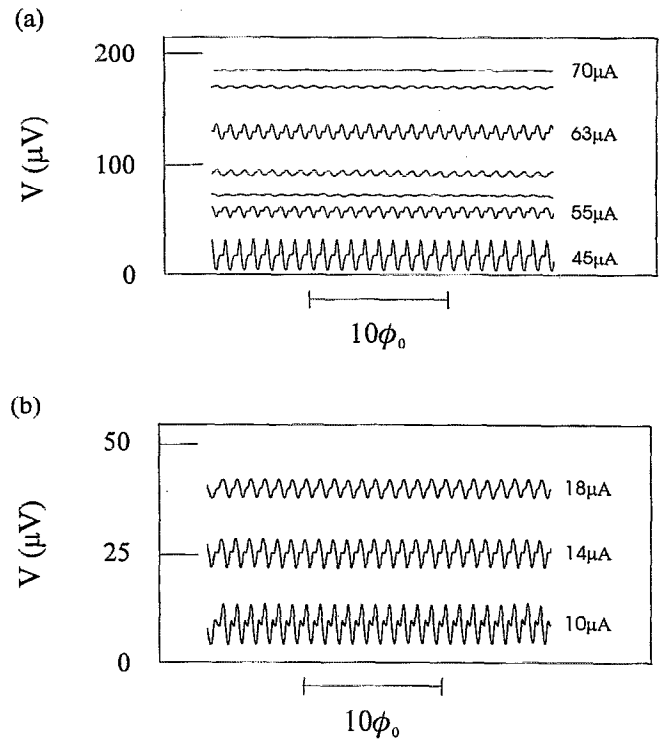


FIG. 3. Voltage vs applied magnetic flux (sample C) for various bias current values at (a) 45 K and (b) 65 K.

good agreement with the values calculated from the geometry.

Although the $V(\phi)$ characteristics are perfectly periodic, they are not smooth. We attribute the kinks in the characteristics to resonances caused by the parasitic capacitance between the input coil and the washer.^{10,11} They may be damped by resistive shunting. Crossing of the $n\phi_0$ and $(n + \frac{1}{2})\phi_0$ branch in the $V(I)$ characteristics, corresponding to a phase shift of $\frac{1}{2}\phi_0$ in the $V(\phi)$ characteristics, is caused by resonant modes in the circuit formed by the junction capacitance and the SQUID inductance.^{12,13} We also observe these so-called beating modes in autonomous dc SQUIDs. The resonances give rise to a current contribution around the voltage $V_{\text{res}} = \phi_0/[2\pi\sqrt{LC/2}]$, with L the SQUID inductance (125 pH and C the junction capacitance. At 45 K the resonance voltage is about 120 μV . From this a specific junction capacitance of 0.2 Fm^{-2} is deduced. This is in agreement with the value obtained from the occurrence of hysteresis.

Temperature-dependent noise measurements were performed on sample C (Fig. 4). The bias current and amplitude of flux modulation were adjusted to minimize the white-noise level. The lowest white-noise level we found was $9.5 \times 10^{-5} \phi_0/\sqrt{\text{Hz}}$, corresponding to $0.17 \text{ pT}/\sqrt{\text{Hz}}$, above 200 Hz at 45 K. A large spread in the amount of low-frequency noise was observed, from $3.5 \text{ pT}/\sqrt{\text{Hz}}$ at 40 K, down to $0.49 \text{ pT}/\sqrt{\text{Hz}}$ at 65 K and 1 Hz. These noise levels are comparable to the values reported earlier for monolithic integrated high T_c SQUID magnetometers,⁶ but higher than

TABLE I. Design parameters of the integrated dc SQUID magnetometers.

	A,B	C
SQUID inductance	125 pH	125 pH
Input coil inductance	7.3 nH	2.3 nH
Mutual inductance	630 pH	360 pH
Pickup loop inductance	15 nH	15 nH
Pickup loop area	56 mm ²	56 mm ²
Expected effective sensing area	1.6 mm ²	1.2 mm ²

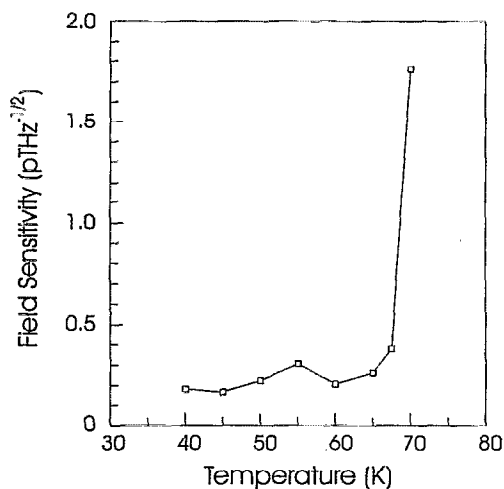


FIG. 4. White-noise level as a function of temperature (sample C). The lowest white-noise level obtained is $0.17 \text{ pT}/\sqrt{\text{Hz}}$ above 200 Hz at 45 K. The low-frequency noise levels showed a large spread. The lowest noise level at 1 Hz was $0.49 \text{ pT}/\sqrt{\text{Hz}}$ at 65 K.

those reported for flip chip magnetometers⁴ and directly coupled magnetometers.³ We attribute these enhanced noise levels to the LC-resonances responsible for the structure in the $V(\phi)$ characteristics. Much improvement of the field sensitivity may be expected if these resonances are damped.

In conclusion, we have fabricated monolithic integrated high T_c dc SQUID magnetometers using a four layer configuration. The first realizations operate up to 73 K. The fabrication process is relatively simple and can easily be

adapted to other types of Josephson junctions. A field sensitivity low enough for many practical applications is obtained. A further improvement of the field sensitivity is foreseen.

The authors would like to thank H. J. Holland and F. J. G. Roesthuis for their technical assistance and A. Kaul and O. V. Snigirev for supplying the BiSrCaCuO shielding. These investigations in the program of the Foundation for Fundamental Research on Matter (FOM) have been supported by the Netherlands Technology Foundation (STW), the OSF, and the National Research Program on High T_c Superconductivity (NOP).

¹ Y. Zhang, M. Mück, K. Herrmann, J. Schubert, W. Zander, A. I. Braginski, and C. Heiden, *IEEE Trans. Appl. Supercond.* **3**, 2465 (1993).

² Y. Tavrín, Y. Zhang, M. Mück, A. I. Braginski, and C. Heiden, *Appl. Phys. Lett.* **62**, 1824 (1993).

³ D. Koelle, A. H. Miklich, F. Ludwig, E. Dantsker, D. T. Nemeth, and J. Clarke, *Appl. Phys. Lett.* **63**, 2271 (1993).

⁴ A. H. Miklich, J. J. Kingston, F. C. Wellstood, J. Clarke, M. S. Colclough, K. Char, and G. Zaharchuk, *Appl. Phys. Lett.* **59**, 988 (1991).

⁵ L. P. Lee, K. Char, M. S. Colclough, and G. Zaharchuk, *Appl. Phys. Lett.* **59**, 3051 (1991).

⁶ R. Kroman, J. J. Kingston, A. H. Miklich, L. T. Sagdahl, and J. Clarke, *Appl. Phys. Lett.* **63**, 559 (1993).

⁷ R. Cantor, T. Ryhänen, D. Drung, H. Koch, and H. Seppä, *IEEE Trans. Magn.* **27**, 2917 (1991).

⁸ D. H. A. Blank, D. J. Adelerhof, J. Flokstra, and H. Rogalla, *Physica C* **167**, 423 (1990).

⁹ J. Flokstra, R. P. J. IJsselstein, and J. W. M. Hilgenkamp, *Thin Solid Films* **218**, 304 (1992).

¹⁰ V. Foglietti, W. J. Gallagher, M. B. Ketchen, A. W. Kleinsasser, R. H. Koch, and R. L. Sandstrom, *Appl. Phys. Lett.* **55**, 1451 (1989).

¹¹ K. Enpuku and H. Koch, *Jpn. J. Appl. Phys.* **32**, 3811 (1993).

¹² Y. Imry and L. S. Schulman, *J. Appl. Phys.* **49**, 749 (1978).

¹³ D. B. Tuckerman and J. H. Magerlein, *Appl. Phys. Lett.* **37**, 241 (1980).